Indoor TDOA-AOA Measurements at the 3G Systems Frequency Band – a Simple Approach

Maurício Henrique Costa Dias, and Gláucio Lima Siqueira, *Member, IEEE*

***Abstract*—This work reports the results of indoor joint AOA-TDOA measurements, using a frequency domain wideband propagation channel sounder (with a vector network analyzer). The whole survey has been carried out in 1.8 GHz, with a 200 MHz bandwidth. Since such kind of sounder only allows the measurement of the channel impulse response, that is, the time-delay spectrum, a synthetic aperture uniform linear antenna array was adopted in order to extend its use to perform also angle-of-arrival measurements. Spatial spectral estimation algorithms such as beamforming, Capon and MUSIC have been applied. The estimated results were compared to expected values, calculated from propagation analysis. Relative errors less than 10% and 35% have been observed in the time-delay and in the spatial domain, respectively. Thus, despite the simplicity, a reasonable performance has been achieved, validating the adopted joint sounding approach.**

***Index Terms*—Propagation channel, wideband channel sounding, angle of arrival, spectral estimation, antenna array.**

Resumo—Este trabalho relata os resultados de medidas conjuntas de AOA e TDOA em ambientes internos, utilizando uma sonda de canal de propagação faixa-larga no domínio da freqüência (com um analisador de rede). O experimento foi realizado na freqüência central de 1,8 GHz, com uma largura de faixa de 200 MHz. Uma vez que este tipo de sondagem só permite a medição da resposta ao impulso do canal, ou seja, do espectro de retardos, um arranjo linear de antenas por abertura sintética foi utilizado para que o espectro espacial (ângulos de chegada) também pudesse ser medido. A estimação do espectro espacial foi feita com base em algoritmos consagrados tais como, por conformação de feixe, Capon e MUSIC. Os resultados estimados foram comparados a valores esperados, calculados a partir de uma análise de propagação. Erros relativos menores que 10% e 35% foram observados nos domínios do retardo e espacial, respectivamente. Portanto, apesar da simplicidade, obteve-se um desempenho razoável, validando a abordagem de sondagem conjunta adotada.

Palavras-Chave—Canal de propagação, sondagem de canal faixa-larga, ângulo-de-chegada, estimação espectral, arranjo de antenas.

Manuscript received April 29, 2005; revised May 19, 2006.

M. H. C. Dias is with the Electrical Engineering Section, Military Institute of Engineering - IME, Rio de Janeiro, RJ, Brazil (phone: 55-21-3820-4135; fax: 55-21-2546-7039; e-mail: mhcdias@ime.eb.br).

G. L. Siqueira is with the Center for Telecommunication Studies (CETUC), Pontifical Catholic University of Rio de Janeiro - PUC-Rio, Rio de Janeiro, RJ, Brazil (e-mail: glaucio@cetuc.puc-rio.br).

I. Introduction

THE present telecommunications scenario points out to an increasing use of indoor mobile systems. Regarding mobile telephony, pico-cellular planning is largely adopted to provide coverage at shopping malls, enterprise buildings and other high-demanding indoor environments. Such strategy has been in practice even before the deployment of the present 3G systems. Wireless LANs (WLANs) also play a major role in that process. The consolidation of HiperLAN2 and IEEE 802.11 standards has created a new wireless "boom". The "hot-spot" concept has broadened even more the spectrum of WLAN potential users, and gives rise to long-term discussions regarding integration issues between 3G and WLAN systems, or even a potential competition between them [1].

One of the greatest challenges to the above-mentioned systems is guaranteeing that the high data transmission rates established may be achieved and sustained. In other words, providing quality of service (QoS) indoors is a complicated task for wideband wireless systems. This is essentially due to the propagation channel behavior, which is random in nature and very difficult to analyze. Small-scale variability is one of the key aspects that needs to be addressed, and it is dictated basically by multipath fading and Doppler spread effects [2].

There are some mitigation techniques widely used to combat multipath fading and Doppler spread. Among the main used are: adaptive equalizing, spread spectrum, channel coding, robust modulation, diversity combining, OFDM, etc. Some of these techniques need to estimate the wideband channel impulse response in order to be effective, like the RAKE receiver for IS-95 systems, for instance [3].

Spatial diversity is being considered to improve the performance of the future communications systems. More specifically, smart antennas and MIMO systems will not only mitigate multipath fading, but will also be able to increase spectrum efficiency [4]-[5]. In this sense, there is a clear need for spatial spectrum estimation techniques [6]-[7], since angle of arrival (AOA) information is used by adaptive processors in those applications. Actually, in the overall, space-time spectrum estimation should be carried out, that is, joint time-delay of arrival (TDOA) and AOA spectrum should be available.

Along the past decade, some joint TDOA-AOA measurements have been reported. The earliest surveys were related to cellular telephony applications, and comprised

ISSN 1980–6604/$20.00

mainly outdoor measurements at the 800-900 MHz and the 1.8-1.9 GHz bands [8]-[10]. As the indoor wireless scenario grew stronger (especially after the year 2000), the main focus of space-time surveys has turned to indoor applications, mainly for WLANs [11]-[15]. However, it is well known that multipath fading tends to be more critical indoors than outdoors. As a result, the most recent indoor surveys reported in the literature adopted more sophisticated estimation techniques, almost always based on maximum likelihood (ML) implementations. In fact, the latter approach provides optimal estimation, though it also presents the highest computational burden among all estimation methods, and it is also subject to convergence problems at some cases [6].

In this context, in which space-time spectrum estimation plays an important role in the present and future communications scene, this work presents the results of a TDOA-AOA survey at a few indoor sites, in the 2,5G and 3G cellular systems frequency band (1.8 GHz). With a single wideband channel sounder available, a simple technique was deployed in order to extend its applicability to allow also AOA estimation. The synthetic aperture concept was adopted in order to synthesize a uniform linear array (ULA) of antennas, thus providing the means to sample the spatial spectrum domain. While the most recent surveys reported [12]-[18] are mainly optimal ML-based approaches, the present work goes on the other hand, trying to show that simpler sub-optimal estimation methods may still be useful, presenting valid results with relatively low computational cost.

This paper is organized as follows. After this introduction section, a brief overview of some classical AOA estimation methods is presented. Next, Section III comprises a review of the main wideband propagation channel sounding techniques, both in the delay and AOA domains. The survey carried out is described in section IV, pointing out details of the sounder setup and of the sites where the measurements have happened. Section V explains the data processing adopted in order to extract space-time spectrum estimates from the available measurements. The estimation results were validated by comparison to expected values calculated from propagation analysis, as described in Section VI. At last, some final remarks are addressed in Section VII.

II. Classical AOA Estimation Methods

The classical AOA estimation methods are simply "spatial" versions of some frequently referred spectral estimation methods. In this work, two non-parametric and one parametric methods are addressed. In the first case, beamforming (or Bartlett) and Capon were chosen, for being among the simplest and widest used non-parametric algorithms. Likewise, MUSIC (*MUltiple SIgnal Classification*) was chosen for being perhaps the most popular among the parametric methods [6]-[7]. The advantage of non-parametric methods is that they do not assume anything about the signals statistical properties. On the other hand, in the cases where such information is available, or at least when it is likely that those properties may be partially assumed, parametric methods may present better performances than the non-parametric ones [6].

An almost ubiquitous hypothesis assumed for the AOA estimation problem is the far-field condition, where the wave fronts are plane, and the array is "far enough" from the source. More specifically, such condition may be analytically described as:

$$\left\{ \begin{array}{c} r > 2D^2 / \lambda \\ r >> \lambda \\ r >> D \end{array} \right\} \tag{1}$$

where r is the separation between the array and the source, D is the maximum dimension of the array (width or height), and λ is the signal wavelength. Fig. 1 illustrates a single signal impinging a ULA of omnidirectional antennas under the far-field condition.

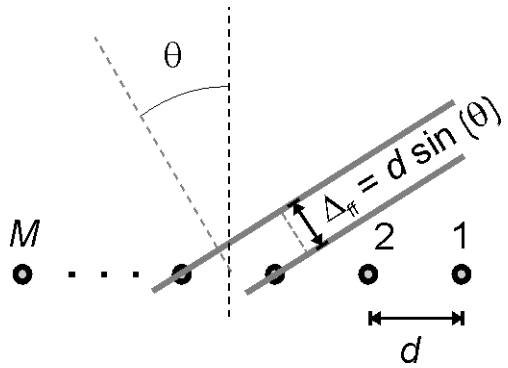

Fig. 1. Uniform linear array of antennas under far-field condition.

In general, classical AOA estimation methods rely on the so-called *array model*, which can be briefly stated as follows [6]. Taking Fig. 1 as reference, if a signal $s(t)$ impinges a M-antennas ULA at an AOA θ, a vector $\mathbf{y}(t)$ is formed on the antennas outputs, such that:

$$\mathbf{y}(t) = \mathbf{a}(\theta)\cdot s(t) + \mathbf{n}(t) \tag{2}$$

$$\mathbf{y}(t) = [\, y_1(t) \cdots y_M(t) \,]^T \tag{3}$$

$$\mathbf{n}(t) = [\, n_1(t) \cdots n_M(t) \,]^T \tag{4}$$

where symbol $\{^T\}$ represents the transposition of a vector or matrix, $y_i(t)$ is the signal at the i^{th} antenna, and $n_i(t)$ is the i^{th} antenna noise, usually considered as white Gaussian distributed. Vector $\mathbf{a}(\theta)$ is frequently known as *steering vector*, and is given by:

$$\mathbf{a}(\theta) = [\, 1 \; \exp(-j\omega_c\tau_2) \; \cdots \; \exp(-j\omega_c\tau_M) \,]^T \tag{5}$$

$$\tau_k = (k-1)\frac{d\cdot\sin(\theta)}{v} = (k-1)\frac{\Delta_{ff}}{v} \tag{6}$$

where ω_c is the signal frequency, τ_k is the far-field TDOA between the k^{th} and the first antennas, d is the spacing between a pair of antennas, Δ_{ff} is the far-field separation between wavefronts impinging consecutive antennas (as in Fig. 1), and v is the phase velocity of the impinging signal. In this model, the *narrowband assumption* is considered.

As it can be noticed in (5) and (6), the steering vector indeed contains the desired AOA information. How such information is "extracted" depends on the specific formulation of each estimation method. It is also worth mentioning that the array model may also be extended to the multipath case. If the impinging signal arrives at the array from L different AOAs, then there will be a steering vector for each direction. If the L $M \times 1$ steering vectors are put together, an $M \times L$ matrix is formed, which is commonly referred as *array manifold*. Thus, the basic array model equation for the multipath case may still be represented by (2), just replacing the steering vector for the array manifold $\mathbf{A}(\theta)$.

Beamforming is an estimation method based on the array model that may be seen as a bank of filters, where each antenna is attributed a weight. If $\mathbf{h}$ is an $M \times 1$ vector comprising the filter weights, the optimization criterion to calculate $\mathbf{h}$ is:

$$\min_{\mathbf{h}} \mathbf{h}^{\mathrm{H}} \cdot \mathbf{h} \quad \text{subject to} \quad \mathbf{h}^{\mathrm{H}} \cdot \mathbf{a}(\theta) = 1 \tag{7}$$

where symbol $\{^{\mathrm{H}}\}$ represents the hermitian of a vector or matrix. The solution to (7) is $\mathbf{h} = \mathbf{a}(\theta)/M$. Thus, summing the outputs of the above-mentioned filters, the power as a function of θ is given by:

$$P(\theta) = \mathbf{a}^{\mathrm{H}}(\theta) \cdot \hat{\mathbf{R}} \cdot \mathbf{a}(\theta) / M^2 \tag{8}$$

where $\hat{\mathbf{R}}$ is an estimate of the signal covariance matrix $\mathbf{R}$, usually taken as:

$$\hat{\mathbf{R}} = \frac{1}{N} \sum_{t=1}^{N} \mathbf{y}(t) \mathbf{y}^{\mathrm{H}}(t) \tag{9}$$

where N is the number of (time) snapshots of the signal available. If the power is calculated for the whole angle domain, a power pattern may be generated. The searched AOA or AOAs will, then, be the angles associated to the main peaks of that pattern.

The beamforming method presents resolution limitation as a function of the number of antennas. The least the number of antennas, the worst the capability to distinguish two or more multipath signals arriving at AOAs very close to each other. However, if such situation is unlikely to happen, or if angular precision is not an issue, this method is adequate enough. Care should also be taken regarding interpretation of the beamforming spectrum, due to the unavoidable presence of undesired sidelobes, especially when multiple AOA estimation is intended [6].

Capon's AOA estimation method calculates the array weights minimizing the mean output power subject to a unity constraint in the look direction θ [19]. In other words, the optimization criterion to calculate $\mathbf{h}$ is:

$$\min_{\mathbf{h}} \mathbf{h}^{\mathrm{H}} \cdot \mathbf{R} \cdot \mathbf{h} \quad \text{subject to} \quad \mathbf{h}^{\mathrm{H}} \cdot \mathbf{a}(\theta) = 1 \tag{10}$$

The solution to (10) is:

$$\mathbf{h} = \mathbf{R}^{-1} \cdot \mathbf{a}(\theta) \Big/ \left\{ \mathbf{a}^{\mathrm{H}}(\theta) \cdot \mathbf{R}^{-1} \cdot \mathbf{a}(\theta) \right\} \tag{11}$$

Again, as in beamforming, summing the outputs of the filters, the power as a function of θ is given by:

$$P(\theta) = \left\{ \mathbf{a}^{\mathrm{H}}(\theta) \cdot \mathbf{R}^{-1} \cdot \mathbf{a}(\theta) \right\}^{-1} \tag{12}$$

The searched AOAs will be associated to the main peaks of the power pattern calculated from (12).

Capon's method is expected to present superior performance compared to beamforming, what is usually confirmed empirically [6]-[7]. On the other hand, a price is paid in terms of computational load, since a matrix inversion operation is needed.

The MUSIC method is a relatively simple and efficient eigenstructure method of AOA estimation [20]. It has many variations and it is perhaps the most studied method in its class. In its standard form, also known as spectral MUSIC, the method estimates the noise subspace from the available samples. This can be done by either eigenvalue or singular value decomposition (SVD) of the estimated data covariance matrix. Once the noise subspace has been estimated, a search for some directions has to be carried out, looking for steering vectors that are as orthogonal to the noise subspace as possible. More specifically, if $\mathbf{R}$ is the signal covariance matrix, it can be eigendecomposed such that:

$$\mathbf{R} = \begin{bmatrix} \mathbf{S} & \mathbf{G} \end{bmatrix} \begin{bmatrix} \lambda_1 & & \\ & \ddots & \\ & & \lambda_M \end{bmatrix} \begin{bmatrix} \mathbf{S}^H \\ \mathbf{G}^H \end{bmatrix} \tag{13}$$

$$\begin{aligned} \mathbf{S} &= \begin{bmatrix} \mathbf{s}_1 & \dots & \mathbf{s}_L \end{bmatrix} \\ \mathbf{G} &= \begin{bmatrix} \mathbf{g}_1 & \dots & \mathbf{g}_{M-L} \end{bmatrix} \end{aligned} \tag{14}$$

where λ_i is an eigenvalue of a $\mathbf{R}$ matrix of rank M, $\mathbf{s_i}$ is a $M \times 1$ vector representing the actual signal subspace, and $\mathbf{g_i}$ is a $M \times 1$ vector representing the noise subspace, with both subspaces orthogonal to each other. Based on such orthogonality, the AOAs may be interpreted as the L sharpest peaks of the following function:

$$P(\theta) = \left\{ \mathbf{a}^{\mathrm{H}}(\theta) \cdot \hat{\mathbf{G}} \cdot \hat{\mathbf{G}}^{\mathrm{H}} \cdot \mathbf{a}(\theta) \right\}^{-1} \tag{15}$$

where $\hat{\mathbf{G}}$ is an estimate of the noise subspace matrix $\mathbf{G}$.

MUSIC usually presents high accuracy and resolution when the actual signal properties are close to the ones assumed *a priori* in the method. For such reason, it is frequently referred to as a "super-resolution" method. On the other hand, a major drawback of this parametric approach is that it assumes the number of the sources (L) as a known parameter, when in fact, knowing that number is an additional estimation problem. Furthermore, compared to the previous methods, MUSIC is also more demanding, numerically speaking, as it requires SVD or eigendecomposition operations.

III. Wideband Propagation Channel Sounding Techniques

A. Wideband TDOA channel measurements

There are three main sounding techniques, as reported in the literature [2], [21]. The eldest one is probably the method that comprises a short duration pulse, trying to simulate the transmission of an ideal impulse. After all, a channel sounding is basically an attempt to measure or estimate the channel impulse response. One of the main problems with this technique is that it is quite subject to interference and noise, due to the wideband filter required [2].

Another sounding technique is the one that takes advantage of the statistical properties of pseudo-random signals, which present impulsive-like autocorrelation functions. Such method is usually referred to as *pulse compression* sounding, and is actually one of the most used techniques nowadays, mainly outdoors. The advantage of this method is that, while the sounding signal may be wideband, it is possible to detect the transmitted signal using a narrowband receiver preceded by a wideband mixer, thus improving the dynamic range as compared to the short pulse sounder. This sounding technique is usually deployed either by the use of a convolution matched-filter or adopting the so-called *swept time-delay cross-correlation* technique (also known as *sliding correlation*) [2], [21].

The third method comprises the frequency domain channel sounding. Fig. 2 illustrates the idea behind this technique, which is most suited for indoor measurements. Basically, the propagation channel (including antennas) is put as device under test (DUT) of a vector network analyzer (VNA). A VNA may provide, among other things, the channel transfer function (equivalent to the S_{21} parameter). With this frequency domain function available, it is just a matter of inverse Fourier transforming that function in order to obtain its time domain equivalent. Such time domain impulse response (IR) represents the channel power distribution as a function of the TDOAs of the multipath arriving signals (relative to the first arriving signal, usually the strongest and main one). For small-scale channel modeling, it is a common practice to calculate the spatial average of the IRs taken over a local area. This average is known as *Power Delay Profile* (PDP) [2]. Despite the difference between the definitions of IR and PDP for a propagation channel, the last term is used indistinctly for both in many references in the literature, since the difference is usually implicit in the context. In the present text, PDP is the term adopted to represent each measured IR.

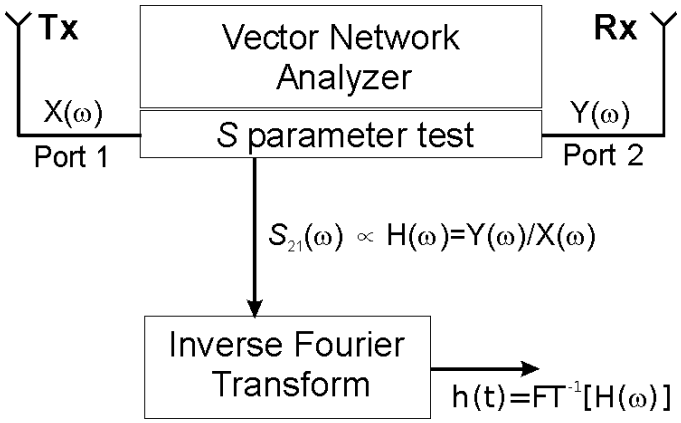

Fig. 2. Concept of frequency domain sounding with a vector network analyzer.

A major limitation of the frequency sounding technique is distance range, since the analyzer ports must be connected to the transmitting and receiving antennas by cables. This is the main reason why this method is more suited to indoor soundings. Another restriction regards the sweep speed of the analyzer within the chosen bandwidth. During the time of a sweep, any channel variations cannot be captured [2].

B. AOA channel measurements

The simplest, yet least efficient, AOA sounding technique is to sweep the angular spectrum with a high gain antenna [22]. Basically it consists on sweeping the angular domain with a highly directive antenna, step by step. At each measurement step, only a small portion of the space surrounding the antenna is actually sounded. The main drawback of this technique is the low achievable resolution, in the order of the antenna beamwidth.

Antenna array processing is the most adopted AOA sounding technique in the present days. It is based essentially on the *array model* previously addressed in Section II. A narrowband signal impinging the array may be sampled a number of times, generating snapshots of the signal vector as in (2). From these snapshots, an estimate of the covariance matrix may be computed, as in (9). With this data matrix available, a convenient spectral estimator must be chosen (beamforming, Capon, MUSIC, etc), and the angular domain must be swept, searching for the spectrum peaks, that will correspond to the AOAs of the impinging signals at the time of the measurement.

Regarding hardware, some significant simplifications may be adopted when deploying an antenna array sounding. A simple, yet highly attractive option is the *synthetic aperture* principle [8]-[10], widely used in radar and remote sensing applications. This method comprises the use of a single antenna (or of a sub-array with small aperture) to carry out the measurements, simply placing the antenna consecutively in

the positions originally expected for a real array. In other words, a *virtual* array is adopted, instead of a real one. Since it takes time to carry out signal sampling along the whole array aperture, this sounding technique has limited capability to track fast AOA channel variations along the time. On the other hand, mutual coupling between the antennas is not an issue, reducing the need for complex angular calibration schemes [12], [22].

Array processing for AOA spectrum estimation requires parallel coherent processing of all the array channels. In other words, ideally, AOA spectrum estimation would require one radio receiver (Rx) per antenna, what may represent a significant burden if the number of antennas is high. A more effective, simpler and cheaper solution is time-division multiplexing of the array outputs. In this way, a single Rx may be used to sequentially capture the channel response at each array element [11]-[12]. As in the synthetic aperture approach, the drawback here is that the sounder will not be able to track fast AOA channel variations as well.

C. Joint space-time channel measurements

Simultaneous space-time channel sounding may be achieved integrating the TDOA and AOA sounding techniques described so far. For instance, an antenna array might be adopted, registering the wideband channel response at each antenna. Wideband TDOA sounding provides the PDP for each antenna of the array, which represents the channel power distribution as a function of the TDOAs of the multipath arriving signals, as previously stated. Thinking of digital processing, the PDP time scale is actually comprised by a finite number of delay bins. Thus, a simple straightforward way to incorporate the AOA spectrum is carrying out the AOA estimation at each delay bin, considering the power distribution in that bin for all antennas of the array. This kind of procedure provides sub-optimal estimation, but the results are still good enough, as reported in the literature [8]-[11].

The above-mentioned approach assumes time channel stationarity along the aperture, that is, from element to element along the array (virtual or not). Considering that usually a relatively small number of array elements is adopted, and that the distance between them is relatively small (less than half wavelength), such hypothesis is actually reasonable enough. In fact, the separation between the array antennas is so small that significant PDP changes are really unlikely to happen. Nonetheless, if the synthetic aperture method or the time-division multiplexing is adopted, small channel variations between the elements may be more evident, since the actual mobile radio propagation channel is only locally stationary [2].

Strictly speaking, true *joint* space-time spectrum estimation requires more sophisticated strategies. In this sense, maximum likelihood (ML) estimation is widely used, especially when parameters have to be estimated from experimental data [23]. ML estimation is usually implemented as iterative numeric methods with high computational burden, and may also present some convergence issues. A practical implementation of ML estimation that has become quite popular in the past few years is the *Space-Alternating Generalized Expectation-maximization* algorithm (SAGE) [24], which was first introduced for channel parameter estimation by Fleury *et al*. [16]. Since then, some SAGE-based soundings have been reported in the literature, mainly for MIMO [14], UWB [25] and 3G systems [18], [26], and also WLANs [13], [15], always presenting very good results.

All in all, the choice for the TDOA-AOA channel sounding approach relies on a tradeoff relationship regarding the estimation method. If accuracy is the main goal and computational burden is not an issue, ML-based algorithms should be adopted. Otherwise, sub-optimal methods may be chosen.

IV. Setup Description

A. Sounder

The whole survey took place in the same locations and dates of another experiment [27], which required ranges up to 150 m along indoor paths. As a result, a frequency domain sounder was adopted, using an optic link as the synchronization device of the employed VNA, instead of a coaxial cable, which would provide shorter ranges (around 50 m). The complete setup is sketched in Fig. 3, and included: a HP8714ET VNA, two 2.14 dBi discone omnidirectional antennas especially built for the 1.8 GHz band, low noise amplifiers, a HP83420A laser, a 500 m multimode encapsulated optical fiber, an optical detector and a desktop computer equipped with a GPIB card for control and data acquisition. The VNA operated with a 200 MHz bandwidth centered at the 1.8 GHz carrier. As a result, the nominal TDOA resolution of the sounder was 5 ns. The setup calibration has been carried out as the one described in [12], storing in the VNA all the unavoidable effects of the system components before each measurement, antennas excluded. The transmitter was chosen to be the mobile unit, since it was the one that consumed less energy, and also in order to keep the fragile laser detector standstill.

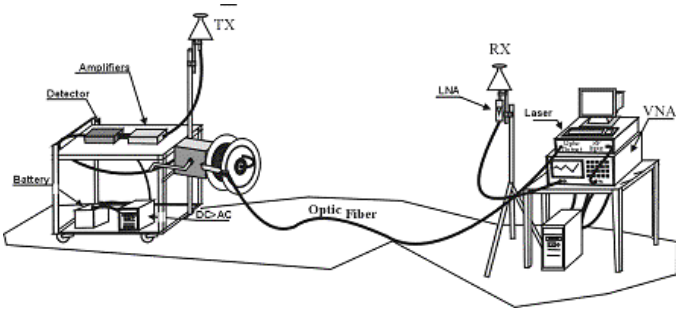

Fig. 3. Illustration of the sounder setup, originally implemented in [27].

The sounder above described was originally deployed for TDOA measurements. In order to extend its use to perform AOA estimation as well, the synthetic aperture concept has been adopted. The spatial sounding comprised only azimuth

variations. Thus, both antennas (transmitter and receiver) were always at the same height (1.7 m above the floor). Since the AOA sounding was one-dimensional, a virtual ULA was chosen, since it is the simplest aperture configuration. Fig. 4 illustrates how the virtual ULA has been synthesized in the present work. It is worth mentioning that, since the virtual array has been formed in the transmitter (Tx) side of the sounder, actually this sounder performed angle of departure (AOD), rather than AOA estimation. Assuming the well-known reciprocity theorem from electromagnetic theory [28], the results of this work hold indistinctly of the link side chosen for the array. Since the array is usually assumed to be at reception in most of the related references, the present work is also described in terms of AOA.

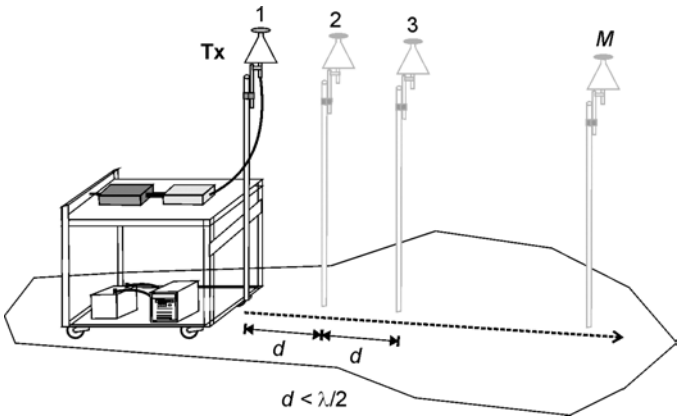

Fig. 4. Virtual ULA implementation – the trolley that carried the transmitter was sequentially placed at the *M* expected array positions.

ULAs present a couple of drawbacks. First, there is a symmetry problem regarding the array axis, such that if two wave fronts impinge the ULA in the same direction, but from opposite senses, these signals cannot be resolved. Second, when non-parametric estimation is carried out, both resolution and detection accuracy present asymmetric behavior, regarding the array's broadside direction. Actually, AOA estimation performance is the best at broadside, and gradually decreases as the AOAs get closer to the endfire direction [6], [29]. The use of planar array geometries (circle, rectangle, etc) solves the first issue, and usually mitigates the latter, at the cost of higher setup complexity [12]-[14].

In digital array processing, the Nyquist sampling theorem is also applicable [6]. More specifically, the spacing between each pair of antennas must be less than ½ wavelength of the impinging signal, in order to avoid (spatial) aliasing. In the survey, a 5 cm separation was adopted, which corresponds to 0.3 of the central carrier wavelength (16.7 cm). The number *M* of elements of the virtual array varied with the sounding site, and it has ranged from 11 to 21 elements. It is worth mentioning at this point that, the greater the array aperture, the better AOA resolution will be. Actually, for beamforming estimation, the relation 1/(*M*-1) defines AOA resolution at the broadside direction [6]. For the other estimation algorithms, AOA resolution is not so simple to derive, but the inverse relation with the array aperture remains.

Since the transmitter antenna had to be relocated for each array position, the survey was limited to standstill AOA soundings. The number of frequency scans (snapshots) at each location was also variable, ranging between 11 and 21.

It should be remarked that the actual aperture synthesis was a rather inaccurate procedure. From Fig. 4 it can be noticed how hard it was to maneuver the trolley supporting the transmitter equipment and antenna, in order to line up the antenna with the expected exact locations of the array elements, which were separated only by 5 cm from each other. Since the main goal of this work was a simple validation of the technique, an accurate antenna positioning control was left for a future improvement of the available setup.

B. Sites

Measurements have been carried out in two different scenarios, both in Rio de Janeiro city. The first site was the second floor of a shopping mall (Gavea). Fig. 5 depicts a blueprint of this site, where stores with glass window facades were present on both sides of the corridors. The receiver was fixed, as well as the virtual transmitting array. Visibility condition was tested at positions "LH" and "LV", which actually referred to the same location and polarization, but with orthogonal alignments (the virtual array at "LH" was perpendicular to the one at "LV"). Such procedure was adopted in order to assess the asymmetric ULA performance (regarding the array's broadside direction) previously discussed. Out-of-sight (OOS) condition was also tested in that site, at the location indicated by an "O" in Fig. 5, which was distant from the Rx location around 25 m in straight line (direct path). Actually, regarding the direct path, a weak obstruction was expected, since the obstructing corner was composed by a thin wood wall with a large glass window.

The measurements took place also inside a building (Leme) of PUC-Rio University. At the fourth floor of Leme building, the transmitter was positioned close to the center of a chosen room, whose door was approximately 30 m apart from the Rx, as pointed out in Fig. 6. As in the mall, the ULA asymmetry has also been tested, taking measurements at orthogonal ULA configurations at the same reference point. ("SH" and "SV"). In this site, only OOS condition was assessed.

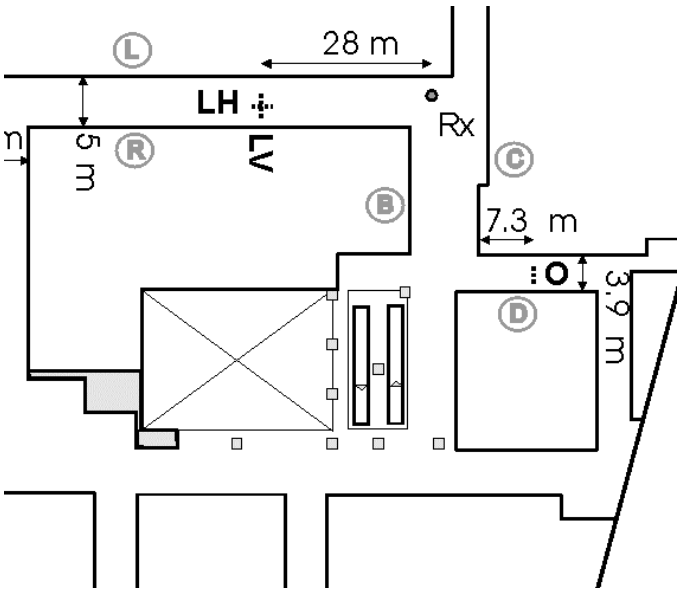

(a)

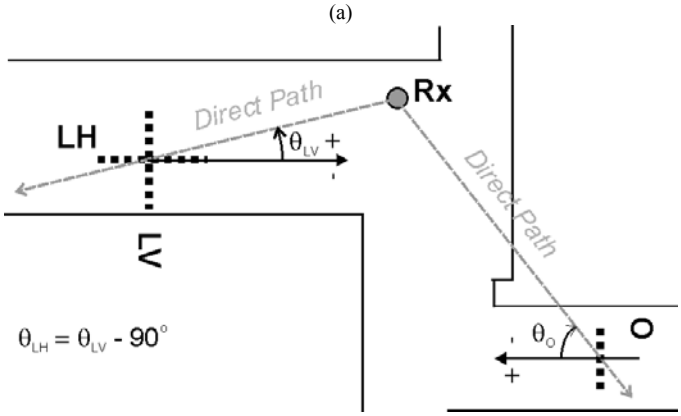

(b)

Fig. 5. (a) Blueprint of the second floor of Gavea mall, pointing out measurement locations, with (b) identification of reference axes for AOAs.

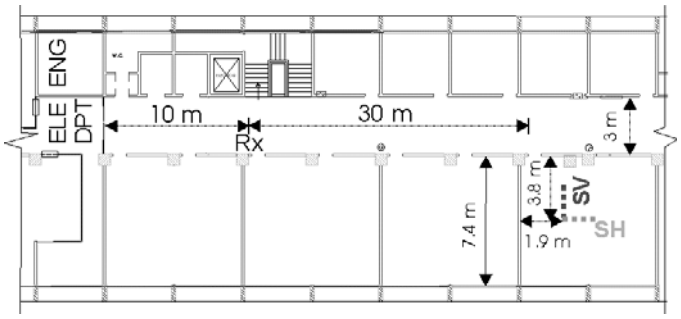

(a)

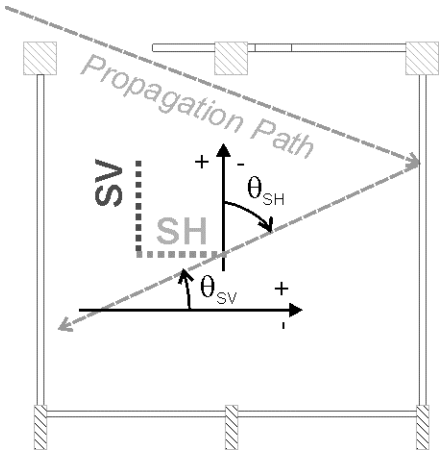

(b)

Fig. 6. (a) Blueprint of the fourth floor of Leme building, pointing out measurement locations, with (b) identification of reference axes for AOAs.

V. Data Processing

The acquisition process has been carried out in real time, during the measurements. A C++ based routine developed for the work in [27] remotely controlled the VNA from the desktop, which stored the sampled data. Each complex transfer function available at the VNA output presented a 200 MHz bandwidth scanning of the propagation channel, which was digitized within a 801 samples window. In average, with that configuration, the setup was able to store two frequency-domain impulse responses (FR) per second. At each one of the five measurement points, the acquisition was done at each array element location, and at each one of these locations a few snapshots were recorded in the computer's hard disk.

The space-time spectrum itself was estimated afterwards, by post-processing, with Matlab® algorithms. The whole post-processing procedure has been realized two-fold. The first block of routines was in charge of generating and organizing the power delay profiles obtained from all the available FRs of a measurement point. This block generated a 3D (three-dimensional) vector of PDPs as output, which was the input to the second block of algorithms. The desired space-time spectrum estimation itself took place in this last block.

Briefly, PDP computation may be summarized as follows. From each FR, a corresponding complex PDP (amplitude and phase) was estimated, computing its correlogram [6]. Such procedure is equivalent to the one adopted in [27], where the inverse discrete fast Fourier transform (IFFT) was taken. Previously to that calculation, a pre-filtering technique was employed, in order to minimize the undesirable spectral leakage imposed by the unavoidable finite number of samples of the FR. The same minimum three-term Blackman-Harris window used in [27] was kept, resulting in a 1.8 width widening for the peaks of the computed PDPs [30]. As a result, the 5 ns TDOA resolution from the original setup was actually decreased to around 9 ns. All of the PDPs calculated as just described for a specific measurement point (comprising *M* array elements and *N* snapshots) were thus rearranged in a 3D vector, with indexes representing delay, time (number of

snapshots) and array element position.

In the second block, after the charge in memory of a 3D vector, the AOA estimation was carried out delay-by-delay. Three distinct AOA estimation methods were adopted in this work: beamforming; Capon; and spectral MUSIC. Basically, from the $M \times N$ data matrix associated to each delay, an estimate of the respective covariance matrix was computed, from which the desired spatial spectral information was extracted, applying any of those estimation methods. MUSIC requires *a priori* information regarding the number of impinging signals (AOAs). In this work, the adopted estimate was the number of peaks of the corresponding beamforming AOA spectrum [29].

It is worth pointing out again that accuracy was not the main concern of this survey. Thus, more refined estimation methods, such as the ML-based previously mentioned [12], [24] which are expected to present better accuracy, have been left out of the assessment. Despite the estimation methods that have been adopted in this work were sub-optimal, its performance is acceptable enough in many cases, as reported in the literature, despite the simplicity and low computational burden behind its implementation [6]-[11].

VI. Sounding Procedure Assessment

A. Methodology

In order to validate the sounding technique, a methodology was adopted, based on a comparison between the estimated results computed from measurements and theoretical AOA expected values, provided from simulation. These expected values were calculated from simple propagation analysis within the survey sites. Actually, since the sounding sites geometries were relatively polygonal, geometrical optics approximation and image theory [28] could have been applied to analyze the main propagation mechanisms. In this work, such mechanisms were direct propagation (associated to the line-of-sight path) and multiple reflections on the walls. Wedge diffraction was not expected to be significant, since the distances were relatively small [31]. Transmission (refraction) through the walls has not been considered in the simulations as well. Such propagation analysis procedure had been previously applied in related works [32], leading to fair agreement with measurements.

The theoretical AOA estimation required knowledge of the angles and distances associated to the main propagation rays. Thus, during the survey, those values have been registered, yet with some inaccuracy level for some data. As a result, an error margin was adopted in this propagation analysis, calculating maxima and minima values of the expected main AOAs and TDOAs when necessary. The expected values were then tabulated in order to be compared to the experimentally estimated ones. Under line-of-sight (LOS) condition, only single reflections have been calculated, besides the direct path. In the other case (OOS), reflections on up to three walls have been considered, and up to 4 times on the same wall when necessary (Leme building site).

All space-time spectra computed have been normalized to their respective power peaks, in order to ease the comparison among the results. Furthermore, path-loss analysis was not intended in the present work.

It should also be mentioned that the main goal of this assessment was a simple validation of the sounder itself. In this sense, TDOA and AOA dispersion analysis could not be carried out, since only a few measurements had been recorded. Serious statistical treatment would require considerably more data.

B. LOS Condition

LOS measurements have been carried out only in the "LH" and "LV" positions of Gavea site, as pointed out in Fig. 5. As expected, the direct path propagation prominence has been confirmed, for all AOA estimation methods tested, as it can be observed in Figs. 7 and 8. Fig. 7 presents the space-time spectrum at point "LV", estimated in the AOA domain by MUSIC, while Fig. 8 presents the space-time spectrum at point "LH", estimated in the AOA domain by beamforming. Since visual identification of the main AOAs and TDOAs from the 3D spectrum is not straightforward at a first glance, two-dimensional (2D) perspectives of both figures are also presented. The main expected AOAs and TDOAs are listed in Tables I and II, for the "LV" and "LH" positions, respectively. Capon estimation could not be computed for point "LH" due to insufficient snapshots available. Those AOAs and TDOAs in the tables may be easily identified at the front and side views of those figures, respectively. As previously mentioned in Section III, the space-time spectrum power peaks occur at the main AOAs and TDOAs. Thus, AOA and TDOA identification is basically a matter of searching the main peaks. Table III presents relative error performance among the three methods, in both points.

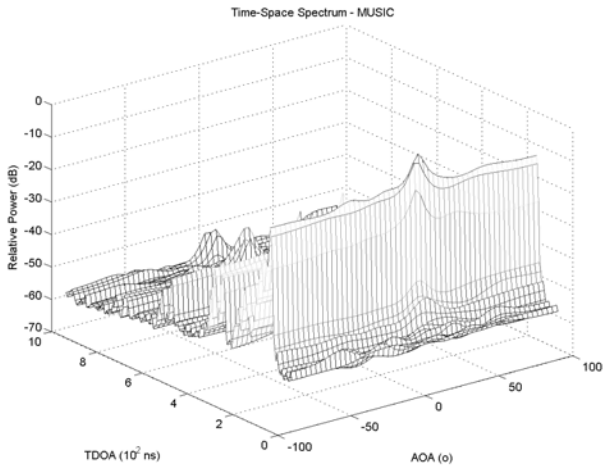

(a)

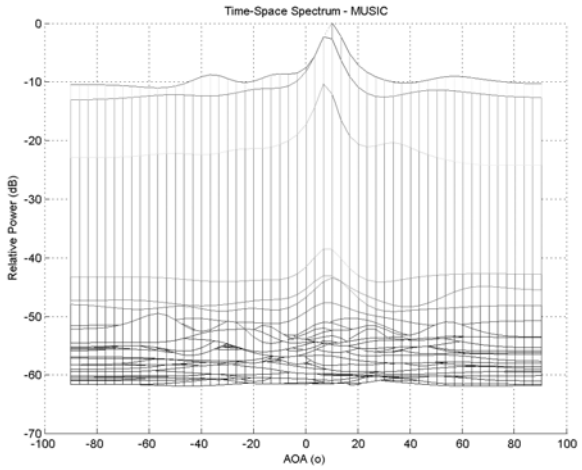

(b)

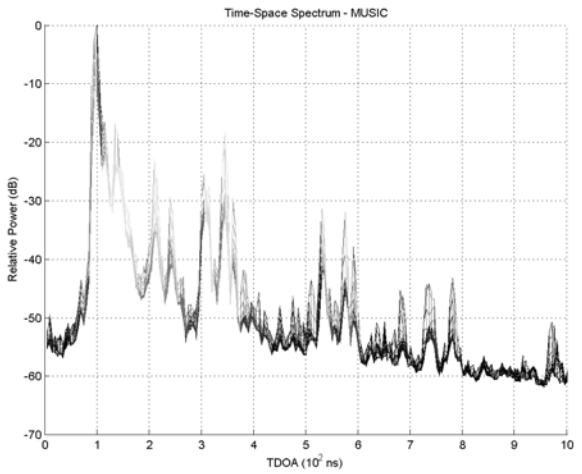

(c)

Fig. 7. MUSIC estimated space-time spectrum in "LV" point: (a) 3D view, (b) front view – AOA spectrum and, (c) side view – TDOA spectrum.

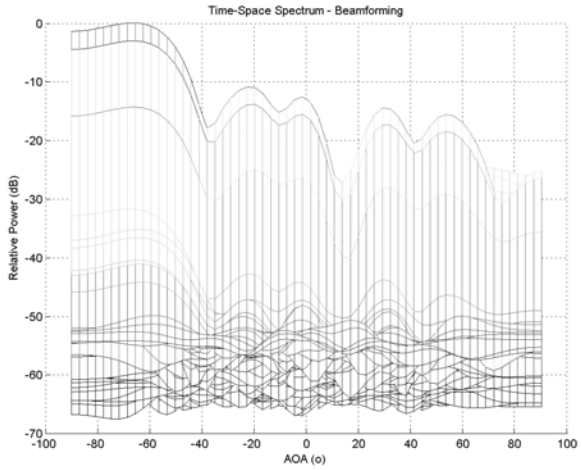

(b)

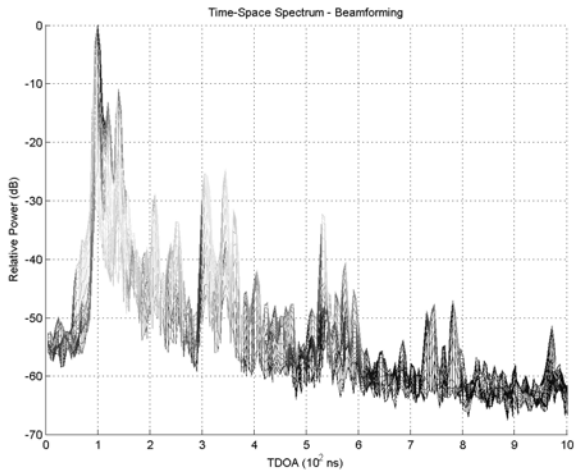

(c)

Fig. 8. Beamforming estimated space-time spectrum in "LH" point: (a) 3D view, (b) front view – AOA spectrum and, (c) side view – TDOA spectrum.

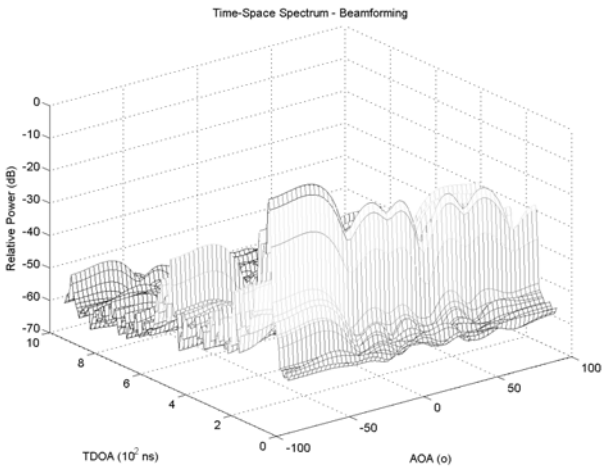

(a)

TABLE I
COMPARISON BETWEEN THE MAIN EXPECTED VALUES AND THE ESTIMATED BY MEASUREMENTS IN "LV" POINT

Path	Expected		Beamforming		Capon		MUSIC	
	θ (°)	τ (ns)	θ (°)	τ (ns)	θ (°)	τ (ns)	θ (°)	τ (ns)
DIR	*1\6*	*93\95*	10	100	10	100	10	100
LR	*8\14*	*94\98*	10	100	10	100	10	100
RR	*-12\-7*	*94\97*	-10	105	-13	105	-10	100

DIR – direct component θ – AOA τ – TDOA
LR – reflection on *L* wall RR – reflection on *R* wall

TABLE II
COMPARISON BETWEEN THE MAIN EXPECTED VALUES AND THE ESTIMATED BY MEASUREMENTS IN "LH" POINT

Path	Expected		Beamforming		Capon		MUSIC	
	θ (°)	τ (ns)	θ (°)	τ (ns)	θ (°)	τ (ns)	θ (°)	τ (ns)
DIR	*-89\-84*	*92\95*	-66	100	--	--	-63	100
LR	*-81\-76*	*94\97*	-66	100	--	--	-63	100
RR	*79\84*	*93\96*	53	100	--	--	75	100

TABLE III
RELATIVE ERROR PERFORMANCE UNDER LOS (%)

Point	Path	Beamforming		Capon		MUSIC	
		Δθ%	Δτ%	Δθ%	Δτ%	Δθ%	Δτ%
"LV"	DIR	185.7	6.4	185.7	6.4	185.7	6.4
	LR	-9.1	4.2	-9.1	4.2	-9.1	4.2
	RR	5.3	9.9	36.8	9.9	5.3	4.7
"LH"	DIR	-23.7	7.0	--	--	-27.2	7.0
	LR	-15.9	4.7	--	--	-19.7	4.7
	RR	-35.0	5.8	--	--	-8.0	5.8

$\Delta\theta\% = 100\ [\theta_{method} - \text{mean}(\theta_{expected})]/\ \text{mean}(\theta_{expected})$
$\Delta\tau\% = 100\ [\tau_{method} - \text{mean}(\tau_{expected})]/\ \text{mean}(\tau_{expected})$

In both points, the couple of single reflected components arrived very close in time to the direct one, and since the nominal delay resolution was 5 ns, it was expected that those three components appeared at the same delay bin, or at most with a single delay bin difference, in the estimated space-time spectra. Moreover, it was expected that none of the methods would be able to resolve the direct component (DIR) from the one reflected on *L* wall (LR), especially beamforming. AOA beamforming resolution (at broadside direction – $\theta = 0^o$) was around 18^o and 20^o for "LH" and "LV", since the arrays had 12 and 11 elements, respectively. In fact, the results shown in Fig. 7 and Fig. 8 confirm that the DIR and LR paths have not been resolved, since only a single peak has been estimated within the angle range in which they were expected. The excessive relative AOA errors seen in Table III for the DIR component in both points are also related to that.

It may be noticed in Figs. 7 and 8 (b) that the AOA dynamic range was low, around 10 dB only. Such relatively poor behavior may be due essentially to the inaccuracies of the adopted sounding procedure (in the AOA domain), which have already been mentioned in Section IV. Adding to that, non-parametric estimation (especially beamforming) inherently suffers from spectral leakage, i.e., undesired sidelobes are present along the spectrum. Clustering effects around the sounder, which have not been considered in the theoretical simulations, also affected the AOA sounding performance in a negative way. Nevertheless, AOA estimation performance was quite reasonable, as indicated in Table III (apart from the DIR path, already discussed).

In the overall, MUSIC presented the best behavior, and the measurements at "LV" were the most accurate. This was actually expected, since MUSIC is known to provide better resolution than non-parametric methods. A price is paid in terms of numerical load, however, since it requires more iterations than its non-parametric counterparts. The best performance for the "LV" point was just a consequence of the asymmetric behavior regarding the array's broadside direction, mentioned in Section IV.

Regarding TDOA estimation, the adopted (TDOA) wideband sounder was actually expected to present good performance, since its calibration and processing schemes were based on previous successful surveys [27]. The relatively high dynamic range (DR) achieved for the PDPs (around 60 dB) was another positive feature that reinforced that expectation. Such good behavior has been confirmed. As it can be seen in Table III, the relative error between the expected and measured TDOAs was less than 10% for all methods, in both points, what can be taken as a good result.

C. OOS Condition

The OOS condition analysis required computation of multiple reflection components. Even so, the direct component was also calculated for the "O" point, due to the weak obstruction expected there. Fig. 9 presents the space-time spectrum for point "O", estimated in the AOA domain by beamforming. The main expected AOAs and TDOAs for that point are listed in Table IV.

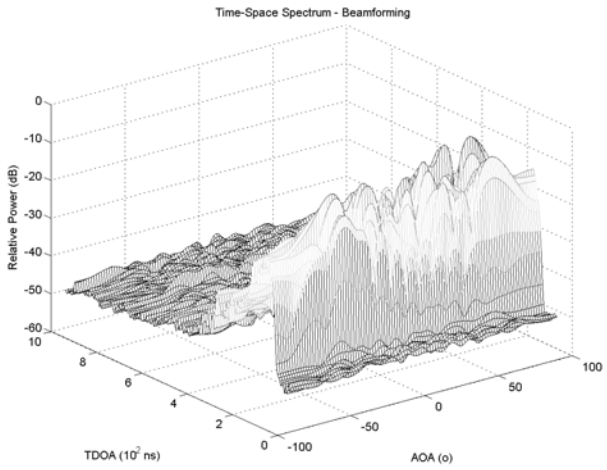

Fig. 9. Beamforming estimated space-time spectrum in "O" point.

TABLE IV
COMPARISON BETWEEN THE MAIN EXPECTED VALUES AND THE ESTIMATED BY MEASUREMENTS IN "O" POINT

Path	*Expected*		*Beamforming*		*Capon*		*MUSIC*	
	θ (°)	τ (ns)	θ (°)	τ (ns)	θ (°)	τ (ns)	θ (°)	τ (ns)
DIR (*)	*-66\-61*	*82\95*	-64	90	-61	90	--	--
BR (*)	*-58\-52*	*91\104*	-50	95	-55	95	-54	100
DR (*)	*65\69*	*95\108*	71	105	69	100	69	105
BR+ DR	*56\61*	*102\115*	52	110	57	115	54	115
CR+ BR+ DR	*44\51*	*119\135*	48	120	42	135	50	120

DIR – direct component BR – reflection on *B* wall * – obstructed path
DR – reflection on *D* wall CR – reflection on *C* wall

As Table IV points out, the estimation in point "O" could have been calculated even for the expected blocked propagation paths. Actually, as previously remarked, since the expected blockage was weak, those blocked components were strong enough to be sensed by the sounder. However, inaccuracy of the available geometrical data was the greatest

of the whole survey. Angle resolution, on the other hand, has not been a critical issue in this analysis. The array synthesized in point "O" had 21 elements, giving the best survey resolution (at broadside), less than 10^o. Moreover, since the expected TDOAs of the main components were sufficiently distinct, that is, separated from each other by more than the 5 ns nominal sounder delay resolution, each component was expected to be found at a distinct delay.

The remaining two measurement sets have been carried out inside a classroom within Leme building, in PUC-Rio campus, as described in Section IV. Both arrays were synthesized with 13 elements (16^o resolution at broadside), and both were thus under OOS condition. However, the blockage condition for points "SV" and "SH" was not only more severe than the one analyzed in the previous site, but also qualitatively different regarding propagation behavior. For instance, the direct path was blocked by many thicker brick walls of the other rooms in between. Regarding reflections, it must be remarked that the room entrance aperture (0.9 m) was narrower than the one present in the mall (3.9 m), and the distance between Tx and Rx was also greater. As a result, reflected rays were only able to get into the room after many bounces along the corridor. The greater the number of reflections, the greater the corresponding attenuation imposed to the propagated signal. Moreover, in cases like this, the geometrical optics approach may not be adequate enough for propagation modeling, since diffraction may also be relevant. Though propagation theories such as Uniform Asymptotic Theory (UAT) [33] could be more adequate, the simplest reflection theory has been kept in the remaining analysis, with a little more flexibility to decide which theoretical rays would enter or not the room.

Fig. 10 presents the space-time spectrum of point "SV", estimated in the AOA domain by Capon, while Fig. 11 presents the space-time spectrum of point "SH", estimated in the AOA domain by MUSIC. The main expected AOAs and TDOAs are listed in Tables V and VI, for the "SV" and "SH" positions, respectively.

A closer look at Tables V and VI points out to a less efficient estimation in point "SH" than in "SV", since accuracy was better in the latter. Moreover, the number of "missing" estimated components was higher for "SH". Actually, since the expected AOAs were closer to the broadside direction (0^o) of its respective array configuration in "SV" point, once again the ULA asymmetry was responsible for the observed effect on the estimation performance.

Table VII presents relative error performance among the three methods, for all OOS points. MUSIC and Capon performed almost alike, better than beamforming, as it can be noticed.

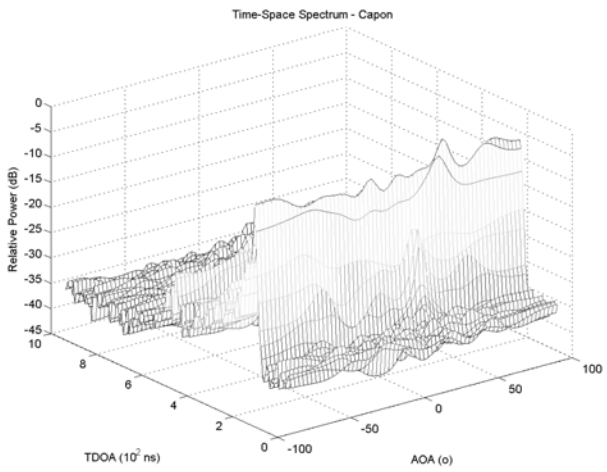

Fig. 10. Capon estimated space-time spectrum in "SV" point.

TABLE V
COMPARISON BETWEEN THE MAIN EXPECTED VALUES AND THE ESTIMATED BY MEASUREMENTS IN "SV" POINT

Path	*Expected*		*Beamforming*		*Capon*		*MUSIC*	
	θ (°)	τ (ns)	θ (°)	τ (ns)	θ (°)	τ (ns)	θ (°)	τ (ns)
C_3R_1	*18\19*	*145*	17	145	17	145	17	145
C_5R_1	*26*	*152/153*	31	155	31	155	34	155
C_6R_1	*29\30*	*157/158*	34	160	34	160	31	160
C_4R_2	*-21\-20*	*160*	-25	160	--	--	--	--
C_3R_2	*-17*	*156*	-8	160	-11	160	-14	160

C_iR_j – *i* reflections along the corridor and *j* within the room.

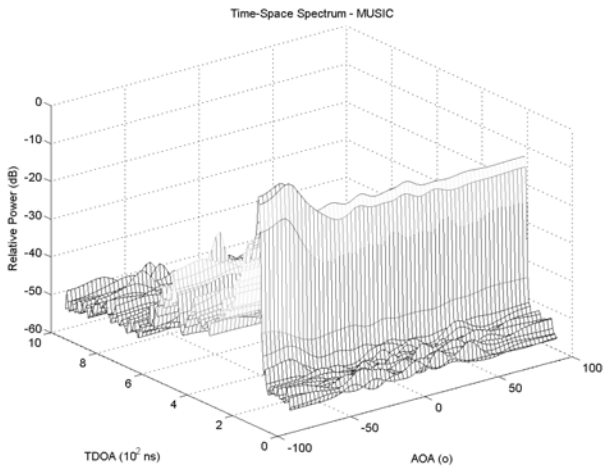

Fig. 11. MUSIC estimated space-time spectrum in "SH" point.

TABLE VI
COMPARISON BETWEEN THE MAIN EXPECTED VALUES AND THE ESTIMATED BY MEASUREMENTS IN "SH" POINT

Path	*Expected*		*Beamforming*		*Capon*		*MUSIC*	
	θ (°)	τ (ns)	θ (°)	τ (ns)	θ (°)	τ (ns)	θ (°)	τ (ns)
C_4R_1	*-67*	*149*	-76	150	-76	150	-76	150
C_5R_1	*-64*	*153*	-76	155	-73	155	-76	155
C_6R_1	*-60*	*156/158*	--	--	-51	160	-45	160
C_3R_2	*73*	*159*	--	--	--	--	68	160

	Expected		*Beamforming*		*Capon*		*MUSIC*	
C_4R_2	*69*	*160/162*	59	165	62	170	59	165

TABLE VII
RELATIVE ERROR PERFORMANCE UNDER OOS (%)

Point	Path	Beamforming		Capon		MUSIC	
		Δθ%	Δτ%	Δθ%	Δτ%	Δθ%	Δτ%
"O"	BR	-9.1	-2.6	0.0	-2.6	-1.8	2.6
	DR	6.0	3.4	3.0	-1.5	3.0	3.4
	BR + DR	-11.1	1.4	-2.6	6.0	-7.7	6.0
"SV"	C_3R_1	-8.1	0.0	-8.1	0.0	-8.1	0.0
	C_5R_1	19.2	1.6	19.2	1.6	30.8	1.6
	C_6R_1	15,3	1,6	15,3	1,6	5,1	1,6
"SH"	C_4R_1	13.4	0.7	13.4	0.7	13.4	0.7
	C_5R_1	18.8	1.3	14.1	1.3	18.8	1.3
	C_6R_1	--	--	-15,0	1,9	-25,0	1,9

VII. CONCLUDING REMARKS

This work addressed the use of a simple technique to carry out joint TDOA-AOA measurements, based on the use of a wideband channel sounder and on the application of the synthetic aperture principle. A survey has been carried out in order to validate that approach, working in the 1.8 GHz frequency band. The experiment took place at five different indoor locations/configurations, comprising both LOS and OOS conditions. The wideband sounder bandwidth was 200 MHz, and a virtual ULA has been adopted. Three distinct AOA spectrum estimation methods have been tested: beamforming, Capon and MUSIC.

Comparison between expected values, calculated from simple propagation analysis, and measurements has been adopted to validate the sounder. In the overall, good agreement has been observed. TDOA estimation performance was expected to be good, since the sounder was able to achieve high TDOA resolution (5 ns nominal - almost 9 ns after windowing) and high dynamic range (60 dB). In fact, the relative errors were low, always within 10%.

AOA estimation performance, on the other hand, was not expected to be that good. After all, a relatively small number of virtual elements was chosen (11 to 21), leading to low AOA resolution (20^o to 10^o, respectively, at most, considering beamforming). Adding to that, the inherent inaccuracies of the array synthesis in the present work, and some undesirable propagation conditions around the sounder (especially clustering) also affected the AOA sounding performance negatively. Even so, apart from a special case in which two propagation components had almost the same AOA, the sounding performance was quite reasonable, with relative errors below 35%, even under OOS. Regarding the AOA estimation algorithm, MUSIC has presented the best behavior under LOS condition, while Capon and MUSIC presented the smallest errors under OOS. Despite having presented the best performance, MUSIC requires more computational resources than the other two tested algorithms.

Comparing the present analysis with related works, it is clear that, if it is possible to add more hardware and software complexity to the sounder, optimal performance may be achieved. Basically, the main improvements should be: the use of planar arrays with as many elements as possible; and choosing more sophisticated spectrum estimation algorithms. True joint space-time spectrum estimation may be achieved with ML-based algorithms, like SAGE [24] and its variations. If an approach similar to the one adopted in the present work is preferred, another sub-optimal AOA estimation method commonly used is ESPRIT (*Estimation of Signal Parameters via Rotational Invariance Techniques*), which is claimed to perform better than MUSIC [6]. Regarding the assessment methodology, full ray-tracing algorithms, including diffracted and refracted rays, may bring more confidence to the analysis. Nevertheless, despite the simplicity, a reasonable performance has been achieved in the present work, thus validating the adopted TDOA-AOA sounding approach.

ACKNOWLEDGMENT

The authors would like to thank all CETUC colleagues who directly contributed to the sounders assembly, and also those who have helped to carry out the measurements.

REFERENCES

[1] W. Lehr and L. W. McKnight, "Wireless Internet access: 3G vs. WiFi?," *Telecommunications Policy*, vol. 27, issues 5-6, pp. 351-370, June-Jul. 2003.

[2] T. S. Rappapport, *Wireless Communications: Principles and Practice*, 2nd ed., Prentice-Hall, 2002.

[3] B. Sklar, *Digital Communications: Fundamentals and Applications*, 2nd ed., Prentice-Hall, 2000.

[4] G. D. Durgin, *Space-Time Wireless Channels*, Prentice-Hall, 2003.

[5] T. S. Rappaport, A. Annamalai, R. M. Buehrer, and W. H. Tranter, "Wireless Communications: past events and a future perspective," *IEEE Communications Magazine*, vol. 40, issue 5 (Part Anniversary), pp. 148-161, May 2002.

[6] P. Stoica and R. Moses, *Introduction to spectral analysis*, Prentice Hall PTR, 1997.

[7] L. C. Godara, *Smart Antennas*, CRC Press, 2004.

[8] J. Fuhl, J. P. Rossi, and E. Bonek, "High-resolution 3-D direction-of-arrival determination for urban mobile radio," *IEEE Transactions on Antennas and Propagation*, vol. 45, issue 4, pp. 672-682, Apr. 1997.

[9] J. P. Rossi, J. P. Barbot, and A. J. Levy, "Theory and measurement of the angle of arrival and time delay of UHF radiowaves using a ring array," *IEEE Transactions on Antennas and Propagation*, vol. 45, issue 5, pp. 876-884, May 1997.

[10] A. Kuchar, J. P. Rossi, and E. Bonek, "Directional macro-cell channel characterization from urban measurements," *IEEE Transactions on Antennas and Propagation*, vol. 48, issue 2, pp. 137-146, Feb. 2000.

[11] R. S. Thomä, D. Hampicke, A. Richter, G. Sommerkorn, A. Schneider, U. Trautwein, and W. Wirnitzer, "Identification of Time-Variant Directional Mobile Radio Channels," *IEEE Transactions on Instrumentation and Measurement*, vol. 49, issue 2, pp. 357-364, Apr. 2000.

[12] R. D. Tingley and K. Pahlavan, "Space-time measurement of indoor radio propagation," *IEEE Transactions on Instrumentation and Measurements*, vol. 50, issue 1, pp. 22-31, Feb. 2001.

[13] C. C. Chong, D. I. Laurenson, C. M. Tan, S. McLaughlin, M. A. Beach, and A. R. Nix, "Joint detection-estimation of directional channel parameters using the 2-D frequency domain SAGE algorithm with serial interference cancellation," in *Proc. IEEE International Conference on Communications (ICC 2002)*, vol. 2, New York – NY, USA, 28 Apr – 02 May 2002, pp. 906-910.

[14] K. Haneda and J. Takada, "High-resolution estimation of NLOS indoor MIMO channel with network analyzer based system," in *14th IEEE Proceedings on Personal, Indoor and Mobile Radio Communications (PIMRC 2003)*, vol. 1, Beijing, China, Sept. 2003, pp. 675-679.

[15] C. C. Chong and D. I. Laurenson, "Spatio-temporal correlation properties for the 5.2 GHz indoor propagation environments," *IEEE Antennas and Wireless Propagation Letters*, vol. 2, pp. 114-117, 2003.

[16] B. H. Fleury, M. Tschudin, R. Heddergott, D. Dahlhaus, and K. L. Pedersen, "Channel Parameter Estimation in Mobile Radio Environments Using the SAGE Algorithm," *IEEE Journal on Selected Areas in Communications*, vol. 17, issue 3, pp. 434-450, Mar. 1999.

[17] B. H. Fleury, X. Yin, K. G. Rohbrandt, P. Jourdan, and A. Stucki, "Performance of a High-Resolution Scheme for Joint Estimation of Delay and Bidirection Dispersion in the Radio Channel," in *Proceedings of the IEEE 55th Vehicular Technology Conference (VTC Spring 2002)*, vol. 1, Birmingham – AL, USA, May 2002, pp. 522-526.

[18] J. Verhaevert, E. Van Lil, S. Semmelrodt, R. Kattenbacht, and A. Van de Capelle, "Analysis of the SAGE DOA parameter extraction sensitivity with 1.8 GHz indoor measurements," in *Proceedings of the IEEE 58th Vehicular Technology Conference (VTC Fall 2003)*, vol. 1, Orlando – FL, USA, Oct. 2003, pp. 69-73.

[19] J. Capon, "High resolution frequency-wavenumber spectrum analysis," *Proceedings of the IEEE*, vol. 57, issue 8, pp. 1408-1418, Aug. 1969.

[20] R. O. Schmidt, "Multiple Emitter Location and Signal Parameter Estimation," *IEEE Transactions on Antennas and Propagation*, vol. AP-34, issue 3, pp. 276-280, Mar. 1986.

[21] D. Parsons, *The Mobile Radio Propagation Channel*, John Wiley & Sons, 1992.

[22] J. C. Liberti Jr and T. S. Rappapport, *Smart antennas for wireless communications*, Prentice Hall, 1999.

[23] S. M. Kay, *Fundamentals of Statistical Signal Processing, Volume 1: Estimation Theory*, Prentice Hall, 1993.

[24] J. A. Fessler and A. O. Hero, "Space-Alternating Generalized Expectation-Maximization Algorithm," *IEEE Transactions on Signal Processing*, vol. 42, issue 1, pp. 2664-2677, Oct. 1994.

[25] K. Haneda, J. I. Takada, and T. Kobayashi, "Experimental evaluation of a SAGE algorithm for ultra wideband channel sounding in an anechoic chamber," in *Conference on Ultrawideband Systems and Technologies*, Kyoto, Japan, May 2004, pp. 66-70.

[26] K. I. Pedersen, P. E. Mogensen, and B. H. Fleury, "A stochastic model of the temporal and azimuthal dispersion seen at the base station in outdoor propagation environments," *IEEE Transactions on Vehicular Technology*, vol. 49, issue 2, pp. 437-447, Mar. 2000.

[27] L. H. Macedo, M. H. C. Dias, R. D. Vieira, J. F. Macedo, and G. L. Siqueira, "Mobile indoor wide-band 1.8 GHz sounding: measurement-based time dispersion analysis," in *Proceedings of the IEEE 55th Vehicular Technology Conference (VTC Spring 2002)*, vol. 1, Birmingham – AL, USA, May 2002, pp. 375-379.

[28] C. A. Balanis, *Advanced Engineering Electromagnetics*, Wiley, 1989.

[29] M. H. C. Dias, *Actual mobile radio propagation channel responses estimates on the spatial and temporal domains*, D.Sc. Thesis, Pontifical Catholic University of Rio de Janeiro, Brazil, Apr. 2003 (in portuguese).

[30] F. J. Harris, "On the use of windows for harmonic analysis with the discrete Fourier transform," *Proceedings of the IEEE*, vol. 66, issue 1, pp. 51-83, Jan. 1978.

[31] M. H. C. Dias and M. S. Assis, "Some Remarks on Urban and Suburban Microcell Propagation," in *Proceedings of the 1998 URSI Commission F International Open Symposium on Wave Propagation and Remote Sensing*, vol. 1, Aveiro, Portugal, Sept. 1998, pp. 224-227.

[32] M. H. C. Dias, G. L. Ramos, and G. L. Siqueira, "Ray-Tracing Analysis of 3.5 GHz Propagation at a Typical Urban Environment," in *Proceedings of the 2001 SBMO/IEEE MTT-S International Microwave and Optoelectronics Conference (IMOC)*, vol. 1, Belém, Brazil, Aug. 2001, pp. 203-207.

[33] R. C. Menendez and S. W. Lee, "On the role of geometrical optics field in aperture diffraction," *IEEE Transactions on Antennas and Propagation*, vol. AP-25, issue 5, pp. 688-695, Sept. 1977.

Maurício H. C. Dias was born in São Paulo – SP, Brazil, in July 1970. He received the degree of telecommunication engineer in 1992 and the M.Sc. degree in electrical engineering in 1998, both from the Military Institute of Engineering (IME), Rio de Janeiro, and the D.Sc degree in electrical engineering from Pontifical Catholic University of Rio de Janeiro in 2003.

Since 1992 he is a Brazilian Army officer, and since 2003 he has been with IME, as teacher and researcher. He has published a few papers and has also presented some articles on brazilian and international conferences. His main present research interests are antennas, wave propagation, electromagnetic compatibility, radio-defined software and space-time signal processing.

Dr Dias is a member of the Brazilian Telecommunications Society (SBrT) since 2003. In 2001, he has been awarded for having presented the best graduate paper on the IEEE International Microwave and Optoelectronics Conference (IMOC 2001), at Belém, Brazil.

Gláucio L. Siqueira (M'89) was born in Belo Horizonte, MG, Brazil, in August 1952. He received the degree of electronics and telecommunication engineer from Pontifical Catholic University, Minas Gerais, the degree of mathematician from Federal University of Minas Gerais in 1977 and 1978, respectively, the M.Sc. degree from the Campinas State University (UNICAMP) in 1982, and the Ph.D. degree in electrical engineering from University College London, U.K., in 1989.

Since 1989, he has been with the Center for Telecommunication Studies (CETUC) at Pontifical Catholic University of Rio de Janeiro (PUC/Rio). He has published several research papers including two IEEE Transactions, and was awarded a number of lecturing distinctions. His research interests include random media propagation, rain-induced attenuation, and mobile radio channel characterization and modeling.